Bond-cluster approximation to the axial next-nearest-neighbor Ising model

James H. Taylor* and J. S. Desjardins
Department of Physics, The University of Rhode Island, Kingston, Rhode Island 02881
(Received 6 February 1984; revised manuscript received 27 April 1984)

The three-dimensional simple-cubic spin-$\frac{1}{2}$ axial next-nearest-neighbor Ising model is studied by means of Kikuchi's cluster-variation method employing a new technique described previously [J. S. Desjardins and O. Steinsvoll, Phys. Scr. **28**, 565 (1983)] for the solution of the general equations of equilibrium. The particular solution employed in this paper is equivalent to Bethe's first approximation and yields a surprisingly rich phase diagram with modulated structures appearing up to a repeat distance of 15 planes (the highest studied). The phase diagram obtained by our technique resembles closely the mean-field, spin-$\frac{1}{2}$ phase diagram of von Boehm and Bak with some significant differences: The second-order boundary of the paramagnetic region is at a significantly lower temperature with a minimum at $|\kappa| \sim 0.4$, where κ is the ratio of the antiferromagnetic to the ferromagnetic coupling constant. In addition, we are able to follow the temperature dependence of the shape of the modulated solutions from the squared-off, low-temperature behavior of Selke and Fisher to the sinusoidal behavior of the high-temperature, mean-field results. The position of our Lifshitz point is in good agreement with previous results, as is the conclusion that transitions between phases are of first order. By contrast, in two dimensions the same approximation completely fails to reproduce reported features of the phase diagram.

I. INTRODUCTION

The vast bulk of work on magnetically modulated structures has been done in two or three dimensions, though very general models have been proposed which cover all integer dimensions. Probably the best known is the axial next-nearest-neighbor Ising (ANNNI) model and its variants, proposed by Elliot[1] and subsequently elaborated by Redner and Stanley,[2] Selke and Fisher,[3] von Boehm and Bak,[4,5] and others. In the ANNNI model, one considers a d-dimensional lattice with ferromagnetic nearest-neighbor interactions and an antiferromagnetic next-nearest-neighbor interaction along one special axis. The ferromagnetic interactions along this special axis need not have the same strength as those in the $(d-1)$-dimensional layers normal to it. Considering a three-dimensional (3D) cubic lattice, the Hamiltonian can be written

$$H=-\tfrac{1}{2}\sum_{xyz}(J_0 S_{x,y,z}S_{x\pm1,y\pm1,z}+J_1 S_{x,y,z}S_{x,y,z\pm1} +J_2 S_{x,y,z}S_{x,y,z\pm2}) , \quad (1)$$

where $J_i>0$ for a ferromagnetic interaction, and the modulations occur along the z axis.

This model has been treated in a variety of ways. Redner and Stanley[2] have performed a high-temperature expansion to obtain the general form of the phase diagram. Selke and Fisher have performed a Monte Carlo simulation to obtain a more detailed diagram[3] as well as a low-temperature expansion.[6] von Boehm and Bak used a mean-field calculation[4] and further calculations which include the effects of interacting solitons.[5] In what follows, we show that this very complicated phase behavior in three dimensions can be reproduced by the method developed in Ref. 7.

II. EQUILIBRIUM EQUATIONS AND METHOD OF SOLUTION

A general method of solution for the equilibrium states of any Ising model has been described in detail in Ref. 7 and only those points germane to the present calculation will be discussed here. The simplest possible entropy beyond the mean-field approximation is based on bonds as basic clusters. To make our bond approximation clear,

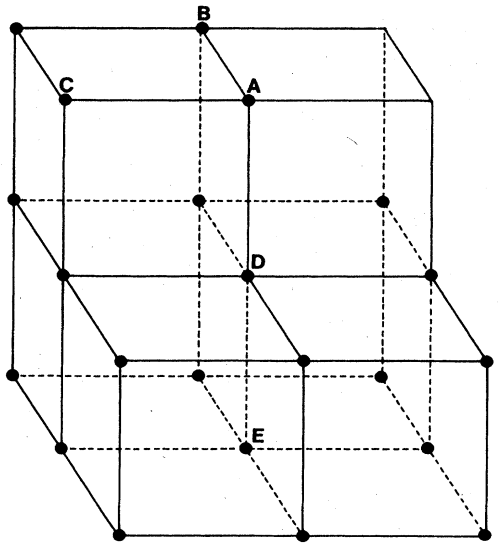

FIG. 1. Approximate entropy construction for the 3D ANNNI model employed in the present calculation. Using Kikuchi's terminology (Ref. 8) lattice point A is placed so as to make the bonds BA, CA, DA, and EA have approximately the "right distribution." EA is a next-nearest-neighbor bond along the chosen axis of magnetization.

refer to Fig. 1, which considers the buildup of a simple-cubic lattice along the 100 direction. In "placing" a typical point A on a given plane we consider points B, C, D, and E to have been already placed.

Since the whole calculation rests on a particular choice of entropy, we transcribe that choice here for reference, using the shorthand notation of the cluster-variation method:[8]

$$\frac{P_B}{B_{AB}}\times\left[\frac{P_C}{B_{AC}}\div\frac{L!}{P_A}\right]\times\left[\frac{P_D}{B_{AD}}\div\frac{L!}{P_A}\right]\times\left[\frac{P_E}{B_{AE}}\div\frac{L!}{P_A}\right]. \tag{2}$$

P and B stand for "point" and "bond" in the language of Ref. 8, while the expression given above denotes the approximate number of ways used by us for placing a typical point A to maintain "right distribution" for an ensemble of L lattices. We now impose the requirement that the magnetization must repeat after m planes along the axis EA in Fig. 1. This necessitates introducing separate magnetization and bond probability variables for each of these planes or distinct pair of planes. A set of Kikuchi relations can be written for each of these which automatically satisfy the lattice sum rules, an essential step in the method:

$$e_1^l=\tfrac{1}{2}+e_l\ ,$$
$$e_2^l=\tfrac{1}{2}-e_l\ ,$$
$$y_1^l=\tfrac{1}{4}+e_l+y_l\ ,$$
$$y_2^l=\tfrac{1}{4}-y_l\ ,$$
$$y_3^l=\tfrac{1}{4}-e_l+y_l\ ,$$

$$2u_1^l=\tfrac{1}{2}+e_l+e_{l+1}+u_l\ ,$$
$$2u_2^l=\tfrac{1}{2}+e_l-e_{l+1}-u_l\ ,$$
$$2u_3^l=\tfrac{1}{2}-e_l+e_{l+1}-u_l\ ,$$
$$2u_4^l=\tfrac{1}{2}-e_l-e_{l+1}+u_l\ ,$$

$$2w_1^l=\tfrac{1}{2}+e_l+e_{l+2}+w_l\ ,$$
$$2w_2^l=\tfrac{1}{2}+e_l-e_{l+2}-w_l\ ,$$
$$2w_3^l=\tfrac{1}{2}-e_l+e_{l+2}-w_l\ ,$$
$$2w_4^l=\tfrac{1}{2}-e_l-e_{l+2}+w_l\ .$$

Here the variables e_l, y_l, u_l, and w_l, $(l=1,2,\ldots,m)$ are the so-called independent variables labeled $x_1,\ldots,x_n$ in Ref. 7. e_1^l is the probability of finding a spin up on any of the planes labeled l with e_2^l the corresponding term for spin down. y_1^l, $2y_2^l$, and y_3^l are the probabilities of finding an up-up, up-down, or down-down neighboring pair within any of the planes labeled l, while u_i^l and w_i^l are the corresponding probabilities for neighboring-plane bonds and next-neighbor-plane bonds along the special axis. We note that each of the bonds is denoted according to the plane of its lower member. The up-down degeneracy of the in-plane bonds is broken for the out-of-plane bonds. As an example of the sum rules satisfied identically, $e_1^l=w_1^l+w_2^l$, etc. Also, in accord with Ref. 7, all the independent variables have been chosen to vanish in the infinite-temperature, random spin state.

Proceeding to the entropy which is essentially the logarithm of the number of ways of arranging the lattice given above, we find that the entropy per site in units of Boltzmann's constant is given by

$$S=\frac{1}{m}\sum_{l=1}^{m}(7E_l-2Y_l-U_l-W_l)\ , \tag{3}$$

where

$$E_l=\sum_{i=1}^{2}e_i^l\ln e_i^l\ ,$$
$$U_l=\sum_{i=1}^{4}u_i^l\ln u_i^l\ ,$$
$$W_l=\sum_{i=1}^{4}w_i^l\ln w_i^l\ ,$$

and

$$Y_l=y_1^l\ln y_1^l+2y_2^l\ln y_2^l+y_3^l\ln y_3^l\ .$$

The configurational energy per site is given by the expression

$$E=-\frac{J_1}{m}\sum_l(2y_1^l-4y_2^l+2y_3^l+u_1^l-u_2^l-u_3^l+u_4^l)$$
$$-\frac{J_2}{m}\sum_l(w_1^l-w_2^l-w_3^l+w_4^l)\ , \tag{4}$$

where the special choice has been made of the same ferromagnetic nearest-neighbor coupling between planes as within planes, and we assume throughout that the external magnetic field is zero. We have considered only the case of J_1 ferromagnetic and J_2 antiferromagnetic. Since each cluster introduces one new independent variable, it is clear from the probability relations that when we look for modulated solutions with a repeat length of m planes, we will be dealing with $4m$ variables, which will require us to solve $4m$ simultaneous nonlinear equations of equilibrium. From Ref. 7 these equations result from minimizing the free energy per site f, where

$$f=\sum_{i=1}^{n}\alpha_i x_i-TS(x_1,\ldots,x_n) \tag{5}$$

and $n=4m$. Here we have ordered the independent variables into a single set $x_1,\ldots,x_n$. In Eq. (5) the dimensionless temperature parameter T is $kT(K)/J_1$ and the function $S(x_1,\ldots,x_n)$ is the entropy per site given by Eq. (3) in units of Boltzmann's constant k. The α_i are obtained from the configurational energy (4) by expressing the probabilities in terms of the independent variables. Minimizing f with respect to the x_i leads to the equilibrium equations

$$\alpha_i/T=\partial S/\partial x_i,\quad i=1,2,\ldots,4m\ . \tag{6}$$

Those x_i values corresponding to $e_1, \ldots, e_m$ are the long-range order parameters; the rest are short range. Our procedure is first to make a choice for m and then to apply our general algorithm[7] for the iterative, simultaneous solution of Eqs. (6) beginning with the known solution at $T=\infty$. A key element in our method is to monitor the eigenvalues of the symmetric matrix $D_{ij}=\partial^2 S/\partial x_i \partial x_j$ evaluated along the solution trajectory $x_1(T)$, $x_2(T), \ldots, x_n(T)$ in the hyperspace of the variables $x_1, \ldots, x_n$. Initially, in the paramagnetic region, the long-range order parameters remain equal to zero along the solution while the short-range order parameters begin to depart from their initial zero values. As the solution proceeds, we can also keep track of the local values of the quantities X_i defined in Eqs. (7) of Ref. 7 as

$$X_i=\sum_{j=1}^{n}\tilde{U}_{ij}x_j \ .$$

Here the orthogonal matrix $U(x_1, \ldots, x_n)$ diagonalizes the D matrix at a point $\vec{x}$ in the hyperspace. Writing the basic differential equation governing the temperature dependence of the solution [Eq. (4) of Ref. 7] in vector form, we have

$$\dot{\vec{x}}=\chi\vec{\alpha} \ ,$$

where

$$\chi=D^{-1}, \quad \dot{\vec{x}}=d\vec{x}/dt$$

and (7)

$$t=1/T \ .$$

Thus

$$\dot{\vec{X}}=\Lambda^{-1}\vec{A}+\dot{\tilde{U}}U\vec{X} \ ,$$

where (8)

$$\vec{A}=\tilde{U}\vec{\alpha} \quad \text{and} \quad \Lambda=\tilde{U}DU \ .$$

Each point along a trajectory defines the position vector $\vec{x}$ of the lattice solution. We imagine that the order parameters $x_1, \ldots, x_n$ are the components of this vector in a fixed coordinate system while the quantities $X_1, \ldots, X_n$ represent the components of this vector in a rotated system of principal axes for which the matrix D_{ij} is diagonal with eigenvalues $\lambda_1, \ldots, \lambda_n$. Similarly $\alpha_1, \ldots, \alpha_n$ and $A_1, \ldots, A_n$ are the components of a second vector, determined by the coupling constants, in the two base systems. As the temperature varies, the principal axes rotate since the matrix $U(\vec{x})$ depends on position. At a critical point, one or more of the eigenvalues making up the diagonal matrix Λ vanish. We will refer to the quantities X_i as the principal order parameters and reserve the term order parameters for the set $x_1, \ldots, x_n$. If A_k/λ_k should diverge at a critical point, Eq. (8) tells us that X_k becomes critical with a divergent temperature derivative. Finally, the heat capacity C and the free energy can be computed along a solution, the former being (in appropriate units)

$$C=-\frac{1}{T^2}\sum_{i=1}^{n}(A_i)^2/\lambda_i \ . \tag{9}$$

We can show that any phase for which every eigenvalue is negative must be considered to be a thermodynamically stable phase, although it may be only metastable. Our criterion is that a stable solution must be an entropy maximum against adiabatic fluctuations in the order parameters. For an arbitrary fluctuation in the order parameters the change in the entropy can be written to second order

$$\delta S=\sum_i(\alpha_i/T)\delta x_i+\tfrac{1}{2}\sum_i\sum_j D_{ij}\delta x_i\delta x_j \ , \tag{10}$$

where use has been made of Eq. (6). Since the first term represents the energy change induced, it vanishes for an adiabatic fluctuation and we are left only with the quadratic term to lowest order. Since we are considering fluctuations around a definite point of solution in $\vec{x}$ space, we may take the U_{ij} matrix elements to be constant and write $\delta\vec{X}=\tilde{U}\delta\vec{x}$. Hence

$$2\delta S=\sum_i\lambda_i(\delta X_i)^2 \ \text{(adiabatic fluctuations)} \ ,$$

and if all the eigenvalues are negative, we may take the phase as stable. All phases selected by us for incorporation into our final phase diagram satisfy this criterion. We will not examine here the question of whether or not it is *necessary* for all eigenvalues to be negative to produce stability. It is clearly sufficient from the argument given above. If several stable phases in the above sense exist at the same temperature, then we have chosen that phase with the lowest free energy to represent the actual state of the lattice.

As we solve Eqs. (6) for decreasing temperature we generally encounter a critical value T_c at which one or more of the eigenvalues vanish. In the case of a second-order phase transition, a bifurcation occurs. It is possible in three dimensions to continue following the unstable, long-range, disordered trajectory below T_c. However, it is also possible to search for a new solution, that is, a new set of x_i which correspond to a long-range ordered phase. Once a set of order parameters is found which is a new solution of (6), one may continue to follow this new trajectory in order-parameter space by our numerical technique described in Ref. 7.

One possibility for finding a new solution below a critical point is to make an orderly scan of the order-parameter space keeping the noncritical principal order parameters fixed while varying only the critical principal order parameters just under T_c. However, a more efficient method has been devised for use with the ANNNI model which takes advantage of an unusual phenomenon that occurs just above T_c. For $T \gg T_c$, the long-range order parameters are zero to within the accuracy of our solutions to Eqs. (6). This means in fact that they are typically $\sim 10^{-20}$ and exhibit no sign of a modulated behavior. As we approach within about 10^{-4} of T_c on the high side a modulated behavior begins to show up in the disordered paramagnetic solution but at a very low level. The order parameters rise from $\sim 10^{-20}$ to $\sim 10^{-10}$ and even though still negligibly small, are plainly modulated. If we follow the disordered curve through T_c these tiny modulations disappear once again far enough below T_c. Since two degenerate eigenvalues vanish together at

the onset of a modulated phase as will be explained in more detail below, we can invariably cause the computer to lock on to the modulated solution below T_c by simply increasing both critical principal order parameters by a factor that multiplies their tiny but well-defined values above T_c to bring them into the range [0.1, 0.4]. All other (noncritical) principal order parameters remain unchanged in this process. Once the proper factor has been found by trial and error, the iteration homes in on the new solution and we can follow it down in temperature. Usually, one or two tries at a multiplying factor is sufficient to bring us onto the new phase trajectory. We have no reason to believe that there could be any actual feedthrough of a modulated solution into the paramagnetic region above T_c and attribute it to a purely numeric effect which proves useful to us when dealing with a large number of independent variables (up to 60). From this it is clear that the grouping of order parameters into the particular linear combinations that represent the principal order parameters is an essential part of our procedure. Obviously, it would be a hopeless task to grope around in a 60-dimensional space for new solutions without a "homing" device of some sort.

III. $T=0$ STATES AND THE ORDERING VECTOR

In three dimensions the eigenvalues form four distinct sets above T_c consisting of m eigenvalues each. There are three sets composed of m degenerate eigenvalues, and one special set in which the eigenvalues occur as degenerate pairs or singlets. If the number of planes m is even, there are two singlets; if odd, only one. The special set always contains the least negative eigenvalue. The eigenvalues in the special set are associated with the long-range order of the system, and the remaining eigenvalues with the short-range order. The m independent long-range order parameters define a subspace of the $4m$-dimensional order-parameter space. This subspace contains the long-range ordering vector. The distribution of the eigenvalues above T_c can be understood as follows, allowing $m=3$ for the sake of clarity. The body diagonals in this 3D Cartesian subspace define four (nonorthogonal) axes. We denote these "zero-temperature" axes. For example, if the long-range ordering vector lies along [111] or $[\bar{1}\,\bar{1}\,\bar{1}]$ the state is ferromagnetic. If instead it lies along $[11\bar{1}]$, the state is modulated in such a way that each plane has the same value of the magnetization but the direction alternates up-up-down, and so on for the other zero-temperature axes. If the vector does not lie on one of these axes, the state is again modulated with a repeat distance of three planes but with differing magnitudes of magnetization on different planes. Any vector lying in the plane orthogonal to the ferromagnetic axis can be described as having components along the other three axes. Since these three axes all correspond to modulated states of "wavelength" $\lambda=3$, there is a natural division of the long-range order eigenvalues into a singlet associated with the ferromagnetic axis, and a pair associated with the two principal axes lying in the orthogonal plane. Similar considerations apply for all values of m. The sets of m equal eigenvalues are associated with short-range ordering involving a specific type of bond.

Above T_c the long-range ordering vector is zero. Just below T_c it grows rapidly within one of the subspaces defined by the different types of ordering already described, each associated with a distinct eigenvalue or eigenvalue pair at T_c. As the temperature decreases, this vector increases in length and rotates toward one of the zero-temperature axes, lying along one of them at $T=0$. As the long-range ordering vector rotates, it must take on components in the different modulated subspaces, each being associated with a different wavelength modulation. Thus, the modulated long-range ordered states take on additional Fourier components as the temperature is lowered, in agreement with Monte Carlo results of Selke and Fisher.[3]

IV. 3D PHASE DIAGRAM

The general program is to assume values for m and κ and then determine the sequence of ordered states that appear as T is decreased by solving Eqs. (6). The resulting phase diagram is shown in Fig. 2. Our Lifshitz point is estimated at $|\kappa| \cong 0.27$ and the region in the near vicinity of this point is shown in the inset. Our notation gives either the simple repeat distance in units of the plane spacing along the special axis or indicates, as for the $\frac{14}{3}$ phase for example, that the modulation undergoes three full cycles in 14 planes. A translation between our notation and its corresponding identification near $T=0$ by Fisher and Selke as the modulation becomes squared off is given in Table I. These identifications have all been made by direct observation of the computer output of each modulated solution from its first appearance in sinusoidal form at T_c down to a sufficiently low temperature to allow an unambiguous identification of its final shape at $T=0$. After observing several of these metamorphoses, one learns rapidly to predict the correct low-temperature form from that of the high temperature as soon as it appears. In this case it has proved very useful to us that our iterative technique will follow any solution and not merely the one with the lowest free energy, since a given modulated solution does not in general remain the most stable one as the temperature is lowered.

By taking constant κ slices sufficiently close to each other and by considering a wide range of m values, we believe that a reasonably accurate phase diagram has been constructed. However, practical considerations of computer time have prevented us from increasing m beyond 15. This made it impossible to locate important longer-wavelength phases. Actually, m would have to be allowed to increase without limit in our method in order to construct a complete phase diagram and, in particular, to study such phenomena as the expected continuous variation of wavelength along the paramagnetic boundary or the occurrence of "devil's staircase" behavior.

The first and most obvious point of consideration for the phase diagram is the $\kappa=0$ slice, which corresponds to the simple nearest-neighbor Ising model. There is only a single transition here, from the high-temperature paramagnetic phase to the ferromagnetic phase at lower temperatures. The value of T_c found by us for $\kappa=0$ is

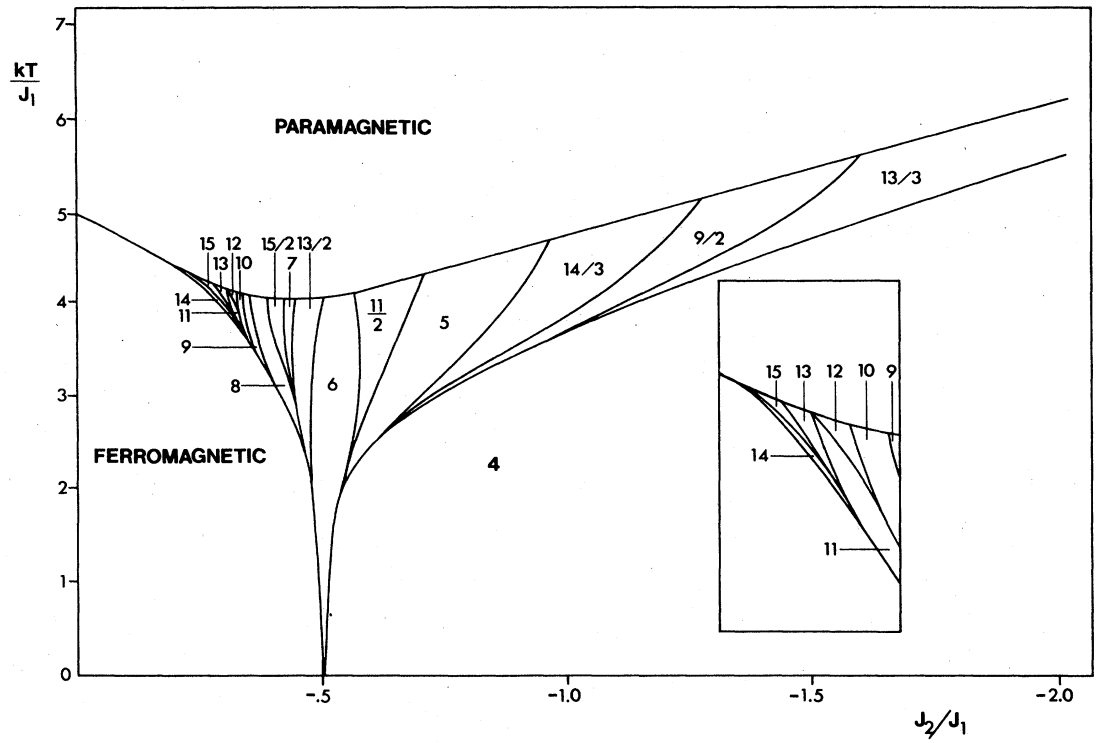

FIG. 2. Resulting 3D phase diagram obtained with the entropy construction of Fig. 1. Integers represent repeat distances of stable phases in units of the lattice constant. Fractions such as $\frac{9}{2}$ indicate two full cycles in nine lattice spacings, etc. Inset shows detail of the phase diagram near the Lifshitz point at $|J_2/J_1| \cong 0.27$. Structures with repeat distance >15 plane spacings were not computed. Table I compares our notation with the corresponding low-temperature, squared-off modulations of Fisher and Selke.

4.9326, the Bethe approximation value for the 3D Ising model. The T_c found here is an improvement over that of von Boehm and Bak, which is equal to 6.[4] Accurate series estimates give a reduced Curie temperature of 4.513.[9]

TABLE I. Translation between Fisher and Selke notation and wavelengths.

Fisher and Selke	Wavelength
$\langle 2 \rangle$	4
$\langle 23 \rangle$	5
$\langle 3 \rangle$	6
$\langle 4 \rangle$	8
$\langle 2^5 3 \rangle$	$\frac{13}{3}$
$\langle 2^3 3 \rangle$	$\frac{9}{2}$
$\langle 2^2 3 \rangle$	$\frac{14}{3}$
$\langle 23^3 \rangle$	$\frac{11}{2}$
$\langle 4^3 3 \rangle$	$\frac{15}{2}$
$\langle 56 \rangle$	11
$\langle 6 \rangle$	12
$\langle 67 \rangle$	13
$\langle 3^3 4 \rangle$	$\frac{13}{2}$
$\langle 34 \rangle$	7
$\langle 45 \rangle$	9
$\langle 5 \rangle$	10
$\langle 7 \rangle$	14
$\langle 78 \rangle$	15

Making an overall comparison of the results obtained here with the phase diagrams of Bak and von Boehm and Fisher and Selke is quite interesting. First, all three phase diagrams indicate the presence of a Lifshitz point. This is a point in the T-versus-κ space at which paramagnetic, ferromagnetic, and sinusoidally modulated phases all coexist. At such a point, the coefficient of the squared-gradient term in the Ginzburg-Landau free-energy functional vanishes.[10,11] Mean-field theory gives a Lifshitz point at $|\kappa| = 0.25$. As mentioned earlier, our analysis yields a value $0.25 \leq |\kappa| < 0.275$, where $|\kappa|$ appears to be closer to the lower bound. Fisher and Selke's second-order estimate for the interfacial tension between the ferromagnetic and $\langle 3 \rangle$ phases gives $|\kappa| \simeq 0.27$ for the Lifshitz point,[12] also, their earlier Monte Carlo study[3] indicates that this is the correct position. There does not appear to be a Lifshitz point for $|\kappa| > \frac{1}{2}$.

The next point of interest is the multiphase point at $T=0$, $|\kappa| = \frac{1}{2}$. Fisher and Selke's low-temperature expansion shows a confluence of an infinity of modulated phases at this point. Their study indicates that, except for the ferromagnetic and $\langle 2 \rangle$ phases, only phases of the type described by the notation $\langle 2^j 3 \rangle$ occur at low temperatures. We find that the phases studied by us of the type $\langle 2^j 3 \rangle$, namely $\frac{13}{3}$, $\frac{9}{2}$, $\frac{14}{3}$, 5, and 6, together with the 4 phase and the ferromagnetic phase, all behave in accord with this confluent result at the multiphase point. For $|\kappa| < \frac{1}{2}$, Refs. 5 and 12 show that the ferromagnetic phase goes directly into the 6 phase at low temperature.

In contrast to the more easily interpreted behavior for $|\kappa| > \frac{1}{2}$, we could not directly verify, for example, that the 8 and $\frac{13}{2}$ phases did not remain stable into the multiphase point. These phases, as well as all the other phases shown in Fig. 2 are, however, degenerate in energy with the $\langle 2^j 3 \rangle$ phases at $T=0$, $|\kappa| = 0.5$.

Bak and von Boehm's soliton-based studies indicate the existence of incommensurable phases at higher temperatures. Our method, due to the built-in choice of repeat distance, is not capable of finding such modulations in its present form.

Duxbury and Selke,[13] using a mean-field approach, have demonstrated the existence of phases of the types $\langle (2^l 3)^m (2^{l+1} 3)^n \rangle$ and $\langle (23^l)^m (23^{l+1})^n \rangle$ at higher temperatures for $|\kappa| > \frac{1}{2}$. Our $\frac{11}{2}$ phase is one of these, and occurs between our 6 and 5 phases, as they predict. Also in agreement with previous work,[4–6] is our bulbous (reentrant) region of 6 phase more or less centered on the $|\kappa| = \frac{1}{2}$ line.

The phase diagram obtained here thus has some of the properties of all of the above-mentioned diagrams, though it seems to resemble most closely Bak and von Boehm's mean-field diagram. This seems quite natural, since the bond approximation is a higher-order mean-field technique. As expected, the lower limit of the paramagnetic region is a line of second-order critical points, while all transitions between modulated phases are of first order.

V. THE TWO-DIMENSIONAL (2D) ANNNI MODEL

The 2D ANNNI model is constructed by simply eliminating one of the dimensions perpendicular to the z axis in the 3D ANNNI model. The Hamiltonian is readily derived from (1), eliminating either the x or y indices from the spins. The system becomes a stack of lines instead of a stack of planes.

Monte Carlo studies by Selke[14] indicate the existence of an incommensurate phase between the $\langle 2 \rangle$ and paramagnetic phases. Also, the Lifshitz point for $|\kappa| < \frac{1}{2}$ disappears. This form for the diagram agrees with a transfer matrix result of Villain and Bak.[15] Findings of Ruján *et al.*,[16] using a variety of techniques, indicate a similar diagram, with the inclusion of a paramagnetic, incommensurately oscillatory region between the ordered incommensurate and strictly paramagnetic regions. This region is characterized by oscillations in the spin-spin correlation function, but not in the magnetization itself.

In view of the incommensurate behavior which has been predicted, it is clear that the approach used by us in three dimensions, which is the main subject of this work, should fail to produce the correct behavior in two dimensions; we look only for commensurate solutions by this method. This expectation was borne out by calculations using a direct adaptation of our previous 3D entropy down to two dimensions; not even the correct $T=0$ behavior was found. This is clearly an extreme example of the effect of dimensionality on a generally accepted method of approximation. Only near $|\kappa| = 0$ do we recover the expected behavior with $T_c = 2.885$ at the ferromagnetic Curie point, compared to 2.268 for the Onsager solution.[9]

ACKNOWLEDGMENTS

One of us (J.H.T.) would like to acknowledge the support of the University of Rhode Island during part of this work. Both of us thank Professor Jill Bonner for her interest, particularly in regard to the situation in the 2D case. This work was supported in part by National Science Foundation (NSF) Contract No. DMR-80-10819.

---

*Present address: Department of Physics, University of Missouri-Rolla, Rolla, MO 65401.

[1]R. J. Elliot, Phys. Rev. **124**, 346 (1961).
[2]S. Redner and H. E. Stanley, Phys. Rev. B **16**, 4901 (1977).
[3]W. Selke and M. E. Fisher, Phys. Rev. B **20**, 257 (1979).
[4]J. von Boehm and P. Bak, Phys. Rev. Lett. **42**, 122 (1979).
[5]P. Bak and J. von Boehm, J. Appl. Phys. **50**, 7409 (1979); Phys. Rev. B **21**, 5297 (1980).
[6]M. E. Fisher and W. Selke, Phys. Rev. Lett. **44**, 1502 (1980).
[7]J. S. Desjardins and O. Steinsvoll, Phys. Scr. **28**, 565 (1983).
[8]R. Kikuchi, Phys. Rev. **81**, 988 (1951); J. Chem. Phys. **60**, 1071 (1973).
[9]D. M. Burley, in *Phase Transitions and Critical Phenomena*, edited by C. Domb and M. S. Green (Academic, New York, 1972), Vol. 2.
[10]W. Selke, Z. Phys. B **27**, 81 (1977).
[11]R. M. Hornreich, M. Luban, and S. Shtrikman, Phys. Rev. Lett. **35**, 1678 (1975).
[12]M. E. Fisher and W. Selke, Philos. Trans. R. Soc. London **302**, 1 (1981).
[13]P. M. Duxbury and W. Selke, J. Phys. A **16**, L741 (1983).
[14]W. Selke, Z. Phys. B **43**, 335 (1981).
[15]J. Villain and P. Bak, J. Phys. (Paris) **42**, 657 (1981).
[16]P. Ruján, Phys. Rev. B **24**, 6620 (1981); G. O. Williams, P. Ruján, and H. L. Frisch, Phys. Rev. B **24**, 6632 (1981).